Title: Temperature controls carbon cycling and biological evolution in the ocean twilight zone

Authors: Flavia Boscolo-Galazzo[1§‡*], Katherine A. Crichton[1§†], Andy Ridgwell [2], Elaine M. Mawbey[3ǂ], Bridget S. Wade[3], Paul N. Pearson[1].

Affiliations:

[1] School of Earth and Environmental Sciences, Cardiff University, Cardiff (UK).

[2]Department of Earth and Planetary Sciences, University of California Riverside, Riverside (USA).

[3]Department of Earth Sciences, University College London, London (UK).

*Correspondence to: flavia.boscologalazzo@uib.no

‡Now at Department of Earth Science, Bergen University and Bjerknes Centre for Climate Research, Bergen (Norway).

†Now at Department of Geography, Exeter University, Exeter (UK).

ǂNow at British Antarctic Survey, Cambridge (UK).

§ Contributed equally to this study

Abstract: Theory suggests that the ocean's biological carbon pump, the process by which organic matter is produced at the surface and transferred to the deep ocean, is sensitive to temperature because temperature controls photosynthesis and respiration rates. Here we apply a combined data-modelling approach to investigate carbon and nutrient recycling rates across the world ocean over the last 15 million years of global cooling. We show that the efficiency of the biological carbon pump increased with ocean cooling due to a temperature-dependent reduction in the rate of remineralization (degradation) of sinking organic matter. Increased food delivery at depth prompted the development of new deep-water niches, triggering deep plankton evolution and the expansion of the mesopelagic "twilight zone" ecosystem.

One Sentence Summary: Earth's temperature affects organic carbon transfer from the surface to the deep ocean, controlling evolution in the "twilight zone".

Main Text: Metabolic temperature-dependency is a physiological response wherein biochemical reaction rates roughly double with an ambient temperature increase of 10°C (*1-5*). On an organismal level, the link between temperature and biochemistry predicts the scaling of metabolism with temperature (*3*). The same relationship has the potential for shaping communities and ecosystems by altering the flux of elements between organisms and the environment (the metabolic theory of ecology) (*1, 2*). A direct implication of this is that biological fluxes of carbon also should scale with temperature as the planet warms or cools. Crucially, because respiration has faster temperature response rates than photosynthesis (*1-5*), more organic carbon should be converted to CO_2 at warmer mean global temperatures, potentially creating a positive feedback to global climate change (*1-6*).

An important component of the global carbon cycle is the ocean's biological carbon pump (BCP) (*7*) in which carbon is fixed at the surface by photosynthesis then transferred down the water column by sinking of particulate organic carbon (POC). Bacterial-driven respiration returns carbon and nutrients to seawater ("remineralization") with the residual organic matter buried in marine sediments (*7-9*). The strength of the BCP is defined as the magnitude of POC settling flux out of the euphotic zone and the transfer efficiency as the fraction of that POC which is transported to greater depths (*10*). Together they determine the efficiency of the BCP in delivering carbon to the deep ocean (*10*). A key controller of the BCP efficiency is the POC remineralization rate: when remineralization is fast, less carbon is transported from the surface to the mesopelagic "twilight zone" (200-1000 m) and deep ocean (*9, 11*).

According to the metabolic theory of ecology (*1, 2*) photosynthesis and POC remineralization rates should be sensitive to secular changes in ocean temperature, modulating the efficiency of the BCP on geological time scales.

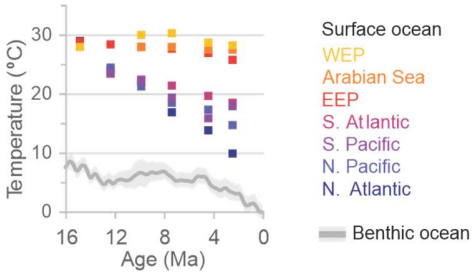

Fig. 1 Global compilation of surface and bottom water temperatures for the last 15 million years. Bottom water temperatures are from (*24*). Surface temperature is presented as a mean value for ocean regions and are compiled from (*19, 20, 22, 43, 44*). WEP is West Equatorial Pacific, EEP is East Equatorial Pacific.

We test this inference, using the rich fossil record of planktonic foraminifera, a group of calcifying heterotrophic protists that live stratified over a range of depth habitats from the surface mixed-layer to thermocline and sub-thermocline intermediate waters (*12*). Foraminiferal shells accumulate on the sea-floor where they retain a geochemical imprint of water-column conditions in which they grew, but which can also be affected by post-depositional alteration (*13*). Previous studies have used foraminiferal shell carbon isotope ratios ($\delta^{13}C$) as means of estimating BCP efficiency, suggesting that it may have been far weaker when climate was much warmer than present such as in the early Eocene, 56-48 million years ago (Ma) (*14, 15*). Modelling has shown that the BCP may have been stronger during glacial maxima (*16*) and could significantly reduce due to ocean warming by the end of the century (*17*). BCP efficiency could have influenced habitability and biological evolution in subsurface marine environments by affecting food supply and levels of oxygen depletion at depth (*18*). However, exploring the sensitivity of the BCP to metabolic temperature dependency and the implications for ocean ecosystems requires extensive datasets across large spatial and temporal scales, which are currently lacking.

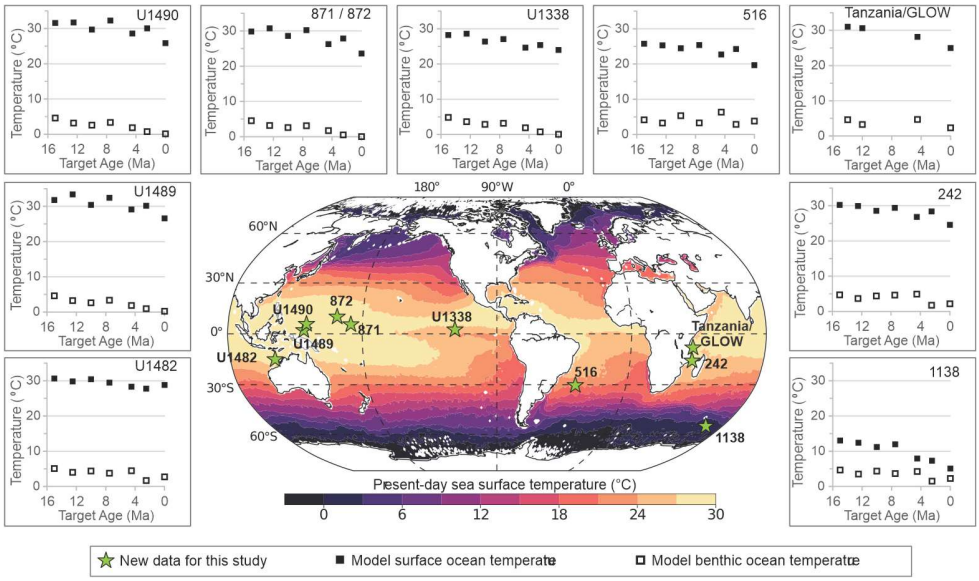

Fig. 2. Modern location of study sites and modelled temperatures. Map shows modern mean annual Sea Surface Temperatures (SST) from World Ocean Atlas 2013 (*45*). Square boxes show surface (filled squares) and bottom (open squares) ocean temperatures as modelled in this study for each location and target age. Sediment core locations are: Deep Sea Drilling Project Sites 242 (western Indian Ocean) and 516 (southwest Atlantic Ocean), Ocean Drilling Program Sites 871 and 872 (western tropical Pacific Ocean) and 1138 (Southern Ocean, Indian Ocean sector), Integrated Ocean Drilling Program Site U1338 (eastern tropical Pacific Ocean), International Ocean Discovery Program Sites U1482 (eastern Indian Ocean), U1489 and U1490 (west Pacific Warm Pool), and hemipelagic sediments collected onshore and offshore Tanzania ("GLOW").

Here we focus on the period since the middle Miocene (15 Ma), over which time there has been a global average temperature decline of between 4 to 6°C in the surface (*19-22*) and deep (*23, 24*) ocean (Fig. 1). Unlike earlier intervals of warming or cooling, it is possible to obtain relevant data from all the ocean basins and across a wide range of latitudes (Fig. 2).

We obtained foraminiferal samples with good to excellent preservation, focusing on seven target ages between 15 and 0 Ma (Fig. 2) (Data S1) (*25*). From these samples we obtained abundance

counts of the different planktonic foraminiferal species and measured the oxygen ($\delta^{18}O$) and carbon ($\delta^{13}C$) stable isotope ratios and Mg:Ca ratios of the shells (Data S2-S4).

With appropriate adjustments for factors such as global ice volume and the local oxygen-isotope composition of seawater, planktonic foraminiferal shell $\delta^{18}O$ can be used as a proxy for relative temperature (*13*), which declines with depth, hence as an indicator of paleodepth ecology (*14*). The $\delta^{13}C$ of near-surface dissolved inorganic carbon (DIC) in the ocean is largely controlled by the ratio between organic matter production by photosynthesis and its destruction by microbial respiration, setting up a $\delta^{13}C$ DIC gradient in the water column (*7, 26*). The $\delta^{13}C$ of planktonic foraminiferal shells is, in turn, controlled by a combination of the isotopic composition of DIC in seawater, and the physiology of biomineralization (*26-29*). Using constrained shell size-fractions, physiological disequilibrium-effects can be minimized and the $\delta^{13}C$ of DIC can be estimated from the shells (*29*). From this, the seawater $\delta^{13}C$ profile can be reconstructed provided that the depth habitats of planktonic foraminifera are also known (*14, 25*) (Fig. 3).

We implemented a series of configurations of the cGENIE Earth system model with appropriate paleogeography and optimized ocean circulation patterns for each target age (Table S1) (*25*, *30, 31*). We further made use of a new version of the model biogeochemistry module that includes temperature-dependent nutrient uptake rates at the surface and respiration in the ocean interior (*32*). This temperature-dependent model configuration ("Tdep") gives rise to profound differences in the physical and biogeochemical properties of the global ocean compared to omitting these processes in the model ("standard") (*32*).

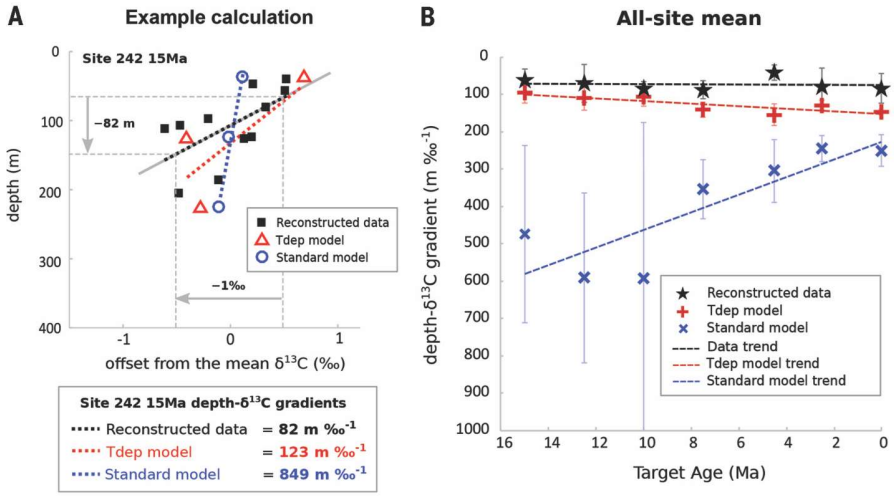

Fig. 3. Comparison of reconstructed and modelled $\delta^{13}C$ DIC gradients. The depth-$\delta^{13}C$ gradient is calculated for: planktonic foraminiferal $\delta^{13}C$ data, the Tdep model, and the Standard model for each target age and site. **(A)** Depth-$\delta^{13}C$ gradients are obtained by calculating the rate of change in $\delta^{13}C$ with depth in the upper 228 m of the water column (*25*). Example calculation of the data and model $\delta^{13}C$ depth-gradients for Site 242 at 15 Ma (see Figs. S2-S3 for all data and model points). In the example, planktonic foraminiferal $\delta^{13}C$ changes by 1‰ in 82 m (indicated by grey dotted lines and grey arrows), the Tdep and Standard model $\delta^{13}C$ decrease of an equivalent amount in 123 and 849 m respectively. **(B)** Reconstructed and modelled depth-$\delta^{13}C$ gradients are summarized as their mean value and one standard deviation of all sites per target age expressed as m $‰^{-1}$ (depth change in meters for 1‰ change in $\delta^{13}C$).

For example, the oldest and warmest middle Miocene (15 Ma) target age is characterized by a much less efficient BCP in the Tdep configuration, with less POC reaching the twilight zone than in the colder Holocene (0 Ma), in accordance with the metabolic theory of ecology (*1*, *2*) (Fig. S1). The Tdep configuration also exhibits higher surface nutrient concentrations due to more vigorous near-surface nutrient recycling across a steeper nutricline, and a shallower oxygen minimum zone in warmer climates (Fig. S1). Combined, this produces a decline in POC export from 15 Ma to the Holocene in the model but a tripling in transfer efficiency, such that there is a net increase in the BCP efficiency on cooling.

To investigate the impact of changes in metabolic rates on the ocean carbon cycle we first identified the average depth habitats of each planktonic foraminiferal species and reconstructed planktonic foraminiferal upper ocean depth-$\delta^{13}C$ gradients as outlined in (*25*) (Fig. 3a). We then contrast our reconstructed depth-$\delta^{13}C$ gradients (*25*) with the results of the standard and Tdep versions of the cGENIE model (Fig. 3b).

At each site, the measured planktonic foraminiferal $\delta^{13}C$ through the upper 228 m (*25*) tends to decrease less with depth from 15 Ma to the present (Figs. S2-S3). As a result, the data-reconstructed global mean depth-$\delta^{13}C$ gradient (expressed in Fig. 3b as m $‰^{-1}$, i.e., depth change in meters for 1‰ change in $\delta^{13}C$), shows a slight trend toward greater depths with cooling (black dashed line in Fig. 3b). In contrast, the standard model (blue dashed line) exhibits a strongly opposite trend (Fig. 3b). Lacking temperature-dependent biological processes in the ocean, the shallowing trend shown by the depth-$\delta^{13}C$ gradient in the standard model (Fig. 3b) is driven by physical climate and ocean circulation changes that result in increasing POC export on cooling. In the Tdep model, the rate of nutrient and carbon cycling in near-surface waters reduces on cooling and counters the "abiotic" trend which results in the nearly muted net projected gradient response. The relatively flat data-reconstructed depth-$\delta^{13}C$ gradient trend is therefore consistent with the hypothesis that carbon remineralization rates in the upper ocean have declined in parallel with global cooling, as characterized in the Tdep model.

We note that even the Tdep model configuration underestimates the reconstructed $\delta^{13}C$ gradient in most cases (Figs. 3b, S2-S3), which may be attributable to the method used to reconstruct $\delta^{13}C$ profiles from the data (*25*), or the various simplifications inherent in the model (*33*).

Most planktonic foraminiferal species in the modern ocean live in the surface mixed layer or upper thermocline around the deep chlorophyll maximum where light is available for photosymbionts and food supply is most abundant (*34*), but some live deeper in the water column, either grazing sinking phytodetritus or predating on mesopelagic organisms such as copepods (*34*). Among this deeper group (colored symbols in Fig. 4) we observe a major deepening of species-specific depth habitats through time which is also reflected by the larger spread in $\delta^{18}O$ and Mg/Ca values in younger target ages (Figs. S4-S8, S9) (Data S3-S4) (*25*). This deepening of habitats coincides with the surface and deep-water cooling shown in global temperature records (Fig. 1). In the older, warmer target ages (15 – 10 Ma) most species lived in the upper 200 m of the water column (Figs. 4, S10). As cooling progressed, subsurface-dwelling species moved to greater depths and new lineages of deep water species evolved. In the most recent target age (0.0 Ma or Holocene) reconstructed depth habitats extend to >1000 m depth (Figs. 4, S10), consistent with observations in the modern ocean (*34*). The deepening pattern is evident in most of the sites, although it is affected by local factors; at the two equatorial sites (Sites U1338 and U1489, Fig. S10) it is complicated by the evolution of the modern zonal temperature gradient between the eastern and western equatorial Pacific Ocean (*19*); at Site U1338 it is also affected by equatorial upwelling (*35*); and at Site 1138 in the Southern Ocean it is obscured by the dominating influence of the subpolar front on the $\delta^{18}O$ of seawater (*36*). Our data emphasize that planktonic foraminiferal species and assemblages have responded in a dynamic way to global climate change and did not occupy constant habitats through time as is sometimes assumed in paleoceanographic reconstructions.

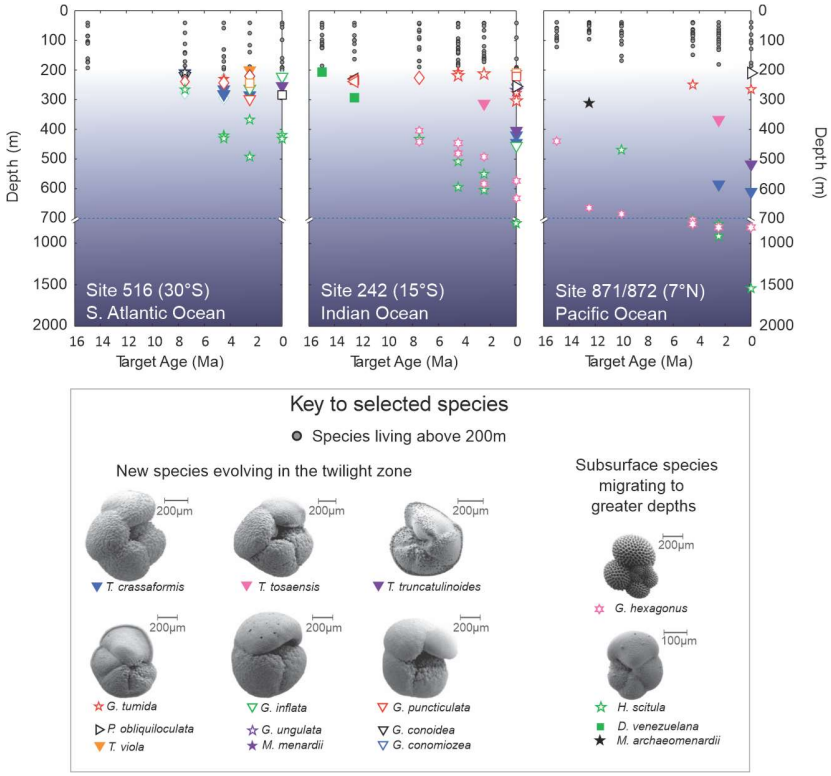

Fig. 4. Expansion of planktonic foraminiferal depth habitat over the last 15 million years. Species in the top 200 m are shown as grey symbols. Deep-dwellers (>200 m reconstructed depth habitat) are highlighted with colored symbols (see Fig. S10 for a complete symbol key). Scanning Electron Microscope images of some mesopelagic planktonic foraminifera from the study sites are also shown. Similar plots for all the study sites are available in Fig. S10.

The global decrease in POC remineralization rate since 15 Ma implies increasing food availability for deep-water organisms that feed directly on POC settling through the water column, and for their associated food chain. Slower remineralization rates of sinking organic matter in the mesopelagic ocean over time would be expected to lead to deeper and less intense oxygen minimum zones (Fig. S1), also favoring organisms which require oxygen for respiration.

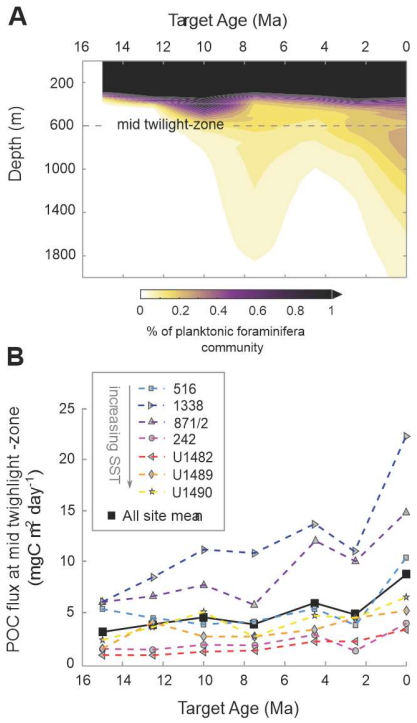

Fig. 5. Abundance depth-distributions of planktonic foraminifera over the last 15 million years. (A) Global mean planktonic foraminiferal community distribution versus time (subpolar Site 1138 not included, see (*25*)); **(B)** Global modelled POC flux for the Tdep model configuration versus time (plotted data are from 600 m depth, the mid twilight zone). Note that not all sites have abundance data for each target age and this explains some of the variability, particularly from 10 to 4.5 Ma.

To investigate whether planktonic foraminiferal biomass reflects increased habitability at depth, we reconstructed the abundance depth-distribution of planktonic foraminiferal assemblages at each site and time slice (*25*) (Data S2) (Figs. S11-S14). Although planktonic foraminifera are always less abundant in deep water than in the euphotic zone, our data show a doubling of biomass in the twilight zone from the middle Miocene to the present (Fig. 5a), paralleled by a more than doubling increase in POC delivery to this region in the Tdep model (Fig. 5b).

These coupled data-modelling results suggest that enhanced food availability was critical for the development of deep plankton niches, as the oceans cooled. Food supply and subsurface oxygen levels are of fundamental importance to all heterotrophs, so we suggest that the mesoplankton and associated nekton as a whole increased in biomass and diversity since 15 Ma. More broadly, the last 15 million years represent the most recent phase in a global cooling trend since the mid-Cretaceous super-greenhouse of ~100 Ma (*37*). Although most of the twilight zone ecosystem leaves no fossil record, temperature-dependency of the BCP may have left a mark on the genetics and phylogenetics of deep-dwelling groups. For instance, the ctenophores (comb jellies), which are common at mesopelagic depths, appear to have a history of recent diversification despite their very ancient (~500 Ma) split from other metazoans (*38*). In addition, various deep-water bony fish clades diversified rapidly since the Miocene (*39-41*) including the extremely abundant lanternfish, which are a dominant proportion of the modern mesopelagic biomass (*41*). Our model results also suggest that since the middle Miocene, a higher proportion of organic carbon fixed at the surface would have reached the sea floor. This fits with previous observations that there has been a marked increase in the abundance of benthic organisms that bloom in response to the deposition of phytodetritus aggregates over this time (*42*).

In summary, our study provides a global test of the effects of temperature changes on metabolic rates in the ocean ecosystem over geological time scales. We found that DIC $\delta^{13}C$ gradients in the upper open ocean changed over the last 15 million years of global cooling in a way that is consistent with reducing remineralization rates and a greater transfer efficiency of the biological carbon pump. Increasing abundance of deep-dwelling zooplankton through the same interval suggests that a more efficient biological carbon pump enhanced the flux of particulate organic carbon to the twilight zone. New ecological niches opened up in response, promoting

evolutionary radiation and the establishment of the modern mesopelagic ecosystem. This evolutionary history raises the possibility that the twilight zone ecosystem may now be vulnerable to a reduction in carbon pump transfer efficiency associated with anthropogenic warming.

References and Notes:

1. J. H. Brown, J. F. Gillooly, A. P. Allen, V. M. Savage, G. B. West, Toward a metabolic theory of ecology. *Ecology* **85**, 1771–1789 (2004).
2. A. P. Allen, J. F. Gillooly, J. H. Brown, Linking the global carbon cycle to individual metabolism. *Funct. Ecol.* **19**, 202–213 (2005).
3. J. F. Gillooly, J. H. Brown, G. B. West, V.M. Savage, E.L. Charnov, Effects of size and temperature on metabolic rate. *Science* **293**, 2248–2251 (2001).
4. B. Chen, M. R. Landry, B. Huang, H. Liu, Does warming enhance the effect of microzooplankton grazing on marine phytoplankton in the ocean? *Limnol. Oceanogr.* **57**, 519–526 (2012).
5. F. Boscolo-Galazzo, K. A. Crichton, S. Barker, P. N. Pearson, Temperature dependency of metabolic rates in the upper ocean: A positive feedback to global climate change? *Global. Planet. Change* **170**, 201–212 (2018).
6. A. Olivarez-Lyle, M. W. Lyle, Missing organic carbon in Eocene marine sediments: is metabolism the biological feedback that maintains end-member climates? *Paleoceanography* **21**, PA2007 (2006).
7. M. P. Hain, D. M. Sigman, G. H. Haug, "The biological pump in the past" in *Treatise on Geochemistry second edition, Volume 8: The Oceans and Marine Geochemistry*, H. D. Holland, K. K. Turekian, Eds. (Elsevier, Amsterdam, 2014) pp. 485-517.
8. P. W. Boyd, H. Claustre, M. Levy, D. A. Siegel, T. Weber, Multi-faceted particle pumps drive carbon sequestration in the ocean. *Nature* **568**, 327-335 (2019)

.

9. E. Y. Kwon, F. Primeau, J. L. Sarmiento, The impact of remineralization depth on the air–sea carbon balance. *Nat. Geosci*. **2**, 630–635 (2009).

10. K. O. Buesseler, P. W. Boyd, E. E. Black, D. A. Siegel, Metrics that matter for assessing the ocean biological carbon pump. *Proc. Natl Acad. Sci. USA* **117***,* 9679–9687 (2020).

11. A. Martin, et all., Study the twilight zone before it is too late. *Nature* **580**, 26-28 (2020).

12. A. Rebotim, A. H. L. Voelker, L. Jonkers, J. J. Waniek, H. Meggers, R. Schiebel, I. Fraile, M. Schulz, M. Kucera, Factors controlling the depth habitat of planktonic foraminifera in the subtropical eastern North Atlantic. *Biogeosciences* **14**, 827-859 (2017).

13. P. N. Pearson, "Oxygen isotopes in foraminifera: Overview and historical review" in *Reconstructing Earth's deep-time climate*, L. Ivany, B. Huber, Eds. Paleontol. Soc. Pap. **18**, 1–38 (2012).

14. E. H. John, P. N. Pearson, H. K. Coxall, H. Birch, B. S. Wade, G. L. Foster, Warm ocean processes and carbon cycling in the Eocene. *Philos. Trans. R. Soc. A*. **371**, 20130099 (2013).

15. E. H. John, J. D. Wilson, P. N. Pearson, A. Ridgwell, Temperature-dependent remineralization and carbon cycling in the warm Eocene oceans. *Palaeogeogr., Palaeoclimatol., Palaeoecol.* **413**, 158–166 (2014).

16. K. Matsumoto, T. Hashioka, Y. Yamanaka, Effect of temperature-dependent organic carbon decay on atmospheric pCO_2. *J. Geophys. Res*. **112**, G02007 (2007).

17. M. Barange, M. Butenschön, A. Yool, N. Beaumont, J. A. Fernandes, A. P. Martin, J. I. Allen, The Cost of Reducing the North Atlantic Ocean Biological Carbon Pump. *Front. Mar. Sci.* **3**, 290 (2017).

18. P. N. Pearson, H. K. Coxall, Origin of the Eocene planktonic foraminifer *Hantkenina* by gradual evolution. *Paleontology* **57**, 243–267 (2014).

19. Y., Zhang, M. Pagani, Z. Liu, A 12-million-year temperature history of the tropical Pacific ocean. *Science* **344**, 84-87 (2014).

20. T. D. Herbert, K. T. Lawrence, A. Tzanova, L. Cleaveland Peterson, R. Caballero-Gill, C. S. Kelly, Late Miocene global cooling and the rise of modern ecosystems. *Nat. Geosci.* **9,** 843–847 (2016).

21. S. M. Sosdian, R. Greenop, M. P. Hain, G. L. Foster, P. N. Pearson, C. H. Lear, Constraining the evolution of Neogene ocean carbonate chemistry using the boron isotope pH proxy. *Earth Planet. Sci. Lett.* **498**, 362–376 (2018).

22. J. R. Super, E. Thomas, M. Pagani, M. Huber, C. O'Brien, P. M. Hull, North Atlantic temperature and pCO_2 coupling in the early-middle Miocene. *Geology* **46**, 519-522 (2018).

23. B. S. Cramer, K. G. Miller, P. J. Barrett, J. D. Wright, Late Cretaceous–Neogene trends in deep-ocean temperature and continental ice volume: Reconciling records of benthic foraminifer geochemistry ($\delta^{18}O$ and Mg/Ca) with sea level history. *J. Geophys. Res*. **116**, C12023 (2011).

24. C. H. Lear, H. K. Coxall, G. L. Foster, D. J. Lunt, E. M. Mawbey, Y. Rosenthal, S. M. Sosdian, E. Thomas, P.A. Wilson, Neogene ice volume and ocean temperatures: Insights from infaunal foraminiferal Mg/Ca paleothermometry. *Paleoceanography* **30**, 1437–1454 (2015).

25. Materials and methods are available as supplementary materials at the Science website.

26. A. Mackensen, G. Schmiedl, Stable carbon isotopes in paleoceanography: atmosphere, oceans, and sediments. *Earth Sci. Rev.* **197,** 102893 (2019).

27. H. J. Spero, D. F. Williams, Extracting Environmental information from planktonic foraminiferal delta-C-13 data. *Nature* **335**, 717–719 (1988).

28. O. Friedrich, R. Schiebel, P. A. Wilson, S. Weldeab, C. J. Beer, M. J. Cooper, J. Fiebig, Influence of test size, water depth, and ecology on Mg/Ca, Sr/Ca, $\delta^{18}O$ and $\delta^{13}C$ in nine modern species of planktic foraminifers. *Earth Planet. Sci. Lett.* **319–320**, 133–145 (2012).

29. H. Birch, H. K. Coxall, P. N. Pearson, D. Kroon, M. O'Regan, Planktonic foraminifera stable isotopes and water column structure: Disentangling ecological signals. *Mar. Micr.* **101**, 127–145 (2013).

30. A. Ridgwell, J. C. Hargreaves, N. R. Edwards, J. D. Annan, T. M. Lenton, R. Marsh, A. Yool, A. Watson, Marine geochemical data assimilation in an efficient Earth System model of global biogeochemical cycling. *Biogeosciences* **4**, 87–104 (2007).

31. K. A. Crichton, A. Ridgwell, D. J. Lunt, A. Farnsworth, P. N. Pearson, Data-constrained assessment of ocean circulation changes since the middle Miocene in an Earth system model. *Clim. Past* https://doi.org/10.5194/cp-2019-151, (2020).

32. K. A. Crichton, J. D. Wilson, A. Ridgwell, P. N. Pearson, Calibration of key temperature-dependent ocean microbial processes in the cgenie.muffin Earth system model. *Geosci. Model Dev*. **14**, 125–149 (2021).

33. D. E. Gaskell, P. M. Hull, Symbiont arrangement and metabolism can explain high $\delta^{13}C$ in Eocene planktonic foraminifera. *Geology* **47**, 1156–1160 (2019).

34. R. Schiebel, C. Hemleben, *Planktic Foraminifers in the Modern Ocean* (Springer-Verlag, Berlin Heidelberg, 2017).

35. L. R. Fox, B. S. Wade, Systematic taxonomy of early–middle Miocene planktonic foraminifera from the equatorial Pacific Ocean: Integrated Ocean Drilling Program, Site U1338. *J. Foramin. Res*. **44,** 374–405 (2014).

36. M. Verducci, L. M. Foresi, G. H. Scott, M. Sprovieri, F. Lirer, N. Pelosi, The Middle Miocene climatic transition in the Southern Ocean: Evidence of paleoclimatic and hydrographic changes at Kerguelen plateau from planktonic foraminifers and stable isotopes. *Palaeogeogr., Palaeoclimatol., Palaeoecol.* **280**, 371–386 (2009).

37. M. Pagani, M. Huber, B. Sageman, "Greenhouse climates" in *Treatise on Geochemistry second edition, Volume 6: The Atmosphere - History*, H. D. Holland, K. K. Turekian, Eds. (Elsevier, Amsterdam, 2014) 281-297 pp.

38. M. Podar, S. H. D. Haddock, M. L. Sogin, G. R. Harbison, A molecular phylogenetic framework for the Phylum *Ctenophora* using 18S rRNA Genes. *Mol. Phylogenet. Evol.* **21**, 218–230 (2001).

39. I. G. Priede, R. Froese, Colonization of the deep sea by fishes. *J. Fish Biol.* **83**, 1528–1550 (2013).

40. T. J. Near, R. I. Eytan, A. Dornburg, K. L. Kuhn, J. A. Moore, M. P. Davis, P. C. Wainwright, M. Friedman, W. L. Smith, Resolution of ray-finned fish phylogeny and timing of diversification. *Proc. Natl Acad. Sci. USA* **109**, 13698–13703 (2012).

41. X. Irigoien, T. A. Klevjer, A. Røstad, U. Martinez, G. Boyra, J. L. Acuña, A. Bode, F. Echevarria, J. I. Gonzalez-Gordillo, S. Hernandez-Leon, S. Agusti, D. L. Aksnes, C. M. Duarte, S. Kaartvedt, Large mesopelagic fishes biomass and trophic efficiency in the open ocean. *Nat. Commun.* **5**, 3271 (2014).

42. E. Thomas, A. J. Gooday, Cenozoic deep-sea benthic foraminifers: Tracers for changes in oceanic productivity? *Geology* **24**, 355–358 (1996).

43. A. Holbourn, W. Kuhnt, M. Regenberg, M. Schulz, A. Mix, N. Andersen, Does Antarctic glaciation force migration of the tropical rain belt? *Geology* **38**, 783-786 (2010).

44. A. E. Shevenell, J. P. Kennett, D. W. Lea, Middle Miocene southern ocean cooling and Antarctic cryosphere expansion. *Science* **305**, 1766-1770 (2004).

45. R. A. Locarnini, A. V. Mishonov, J. I. Antonov, T. P. Boyer, H. E. Garcia, O. K. Baranova, M. M. Zweng, C. R. Paver, J. R. Reagan, D. R. Johnson, M. Hamilton, D. Seidov, *World Ocean Atlas 2013, Volume 1: Temperature,* S. Levitus, A. Mishonov, Eds. (NOAA Atlas NESDIS 73, 2013).

46. Zenodo DOI: 10.5281/zenodo.4469673

47. Zenodo DOI: 10.5281/zenodo.4469678

Acknowledgments: We thank Laura Cotton and Chris Nicholas for collecting the Tanzania surface samples, and the Tanzania Commission for Science and Technology for research permission. We thank Marcin Latas for assisting with sample preparation. We thank the International Ocean Discovery Program for supplying samples for this study. This research used samples provided by the International Ocean Discovery Program (IODP), *JOIDES* Resolution, Expedition 363, West Pacific Warm Pool. This research also used samples provided by Netherlands Organisation for Scientific Research (NWO), RV *Pelagia*, Paleogene GLObal Warming ("GLOW") expedition. Constructive reviews from the Editor, Jesse Farmer, and two anonymous reviewers greatly benefited the manuscript. **Funding:** FBG and KAC were supported by Natural Environment Research Council (NERC) grant number NE/N001621/1 to PNP. PNP was supported by NERC grant NE/P016375/1 to participate to IODP Expedition 363, and by NERC grant NE/F523293/1 for the "GLOW" Expedition. AR acknowledges additional support from the National Science Foundation under Grants 1702913 and 1736771 as well as from the Heising Simons Foundation. EMM was supported by NERC grant NE/N002598/1 to BSW. Marcin Latas was funded through an EU Career Integration Grant 293741 to BSW. **Author contributions: Conceptualization:** PNP; **Software:** KAC; **Formal analysis:** KAC; **Investigation:** FBG, EMM; **Resources:** FBG; **Writing - Original Draft:** FBG; **Writing - Review & Editing:** FBG, KAC, PNP, AR, BSW, EMM; **Visualization:** FBG, KAC, EMM; **Supervision:** PNP, AR, BSW; **Project administration:** PNP, BSW; **Funding acquisition:** PNP, BSW. **Competing interests:** Authors declare no competing interests. **Data and materials availability:** All data are available in the supplementary materials, the code for the version of the "muffin" release of the cGENIE Earth system model used in this paper, is tagged as v0.9.18 and has is assigned a DOI: 10.5281/zenodo.4469673[46]. Configuration files for the specific

experiments presented in the paper can be found in the directory: genie-userconfigs/MS/boscologalazzoetal.2021. Details on the experiments, plus the command line needed to run each one, are given in the readme.txt file in that directory. All other configuration files and boundary conditions are provided as part of the code release.

A manual detailing code installation, basic model configuration, tutorials covering various aspects of model configuration and experimental design, plus results output and processing, is assigned a DOI: 10.5281/zenodo.4469678[47].

Supplementary Materials:

Materials and Methods

Figures S1-S16

Tables S1

External Databases S1-S5

References (*48-67*)